Module 3 : Molecular Spectroscopy
Lecture 15 : Other spectroscopic methods

Objectives

After studying this lecture, you will be able to

- Outline the principles involved in Mossbauer spectroscopy.
- Distinguish between the features of Mass spectrometry, X-ray diffraction and the other spectroscopic methods.
- Outline the use of laser pulses in time resolved/ultrafast spectroscopy.
- Distinguish between Raman spectroscopy and the vibrational spectroscopy of dipolar molecules.
- Distinguish between NMR and NQR.
- Predict the mass spectrum of some simple compounds

15.1 Introduction

So far we have studied standard spectroscopic methods involving transitions amongst molecular rotational, vibrational, electronic and nuclear and electron spin energy levels. There are several other techniques, as well as newly emerging methods which enable one to study other details of molecules as well as allow us to study molecules as a function of time, i.e., as a molecule goes from one state to another.Time resolutions of a femtosecond 10^{-15}s have been accomplished. The development of pulsed lasers has contributed phenomenally to this progress. In the present lecture we shall explore a few more spectral techniques so as to see which other aspects of molecular behaviour can be probed. Some topics covered in this lecture are Mossbauer spectroscopy, nuclear quadrupole resonance (NQR) spectroscopy,Raman spectroscopy, mass spectroscopy/spectrometry. X ray crystallography or mass spectroscopy do not strictly involve transitions between molecular energy levels. Nevertheless, they give complementary useful information on the structure of molecules.

15.2 Mossbauer Spectroscopy

Mossbauer spectroscopy involves the absorption of γ - rays (photons of frequency 10^{19} Hz or wavelengths of 10 pm). The method uses the Mossbauer effect which is the recoilless emission and resonant absorption of γ - rays. A typical energy level diagram involved in a Mossbauer spectrum and a block diagram of the corresponding spectrometer is shown below:

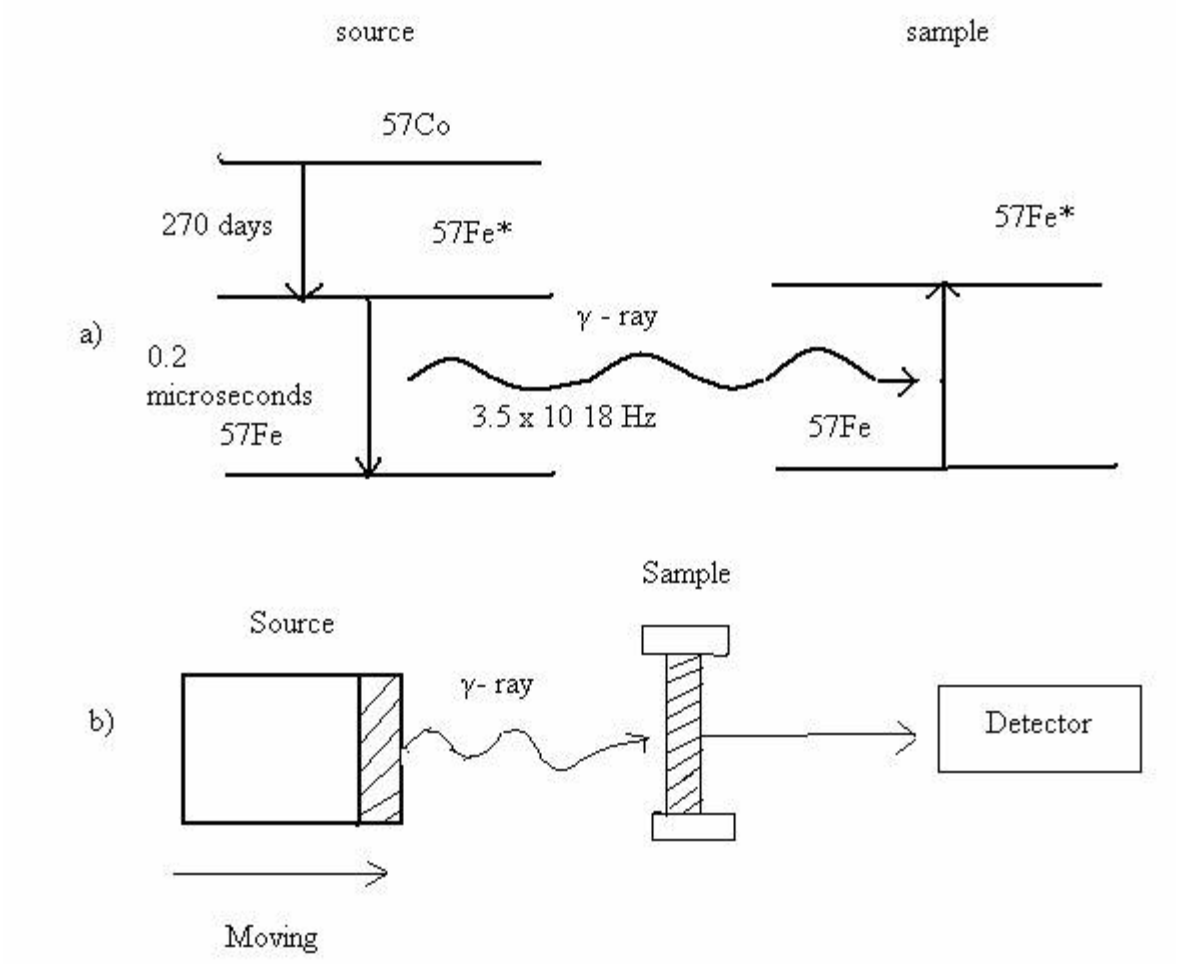

a) Energy levels b) Mossbauer spectrometer

Figure 15.1. Energy levels (a) and a block diagram (b) for Mossbauer spectroscopy

The isotope ^{57}Co decays slowly (half life $t_{½}$ = 270 days) to ^{57}Fe*. ^{57}Fe* has a very short $t_{½}$ (0.2 μs). Corresponding to this half life, the uncertainty in energy is $\Delta E = \hbar t_{½} =$ 2 MHz. A γ - ray of n = 3.5 x 10^{18} Hz (or E = 14.4 keV) is emitted by ^{57}Fe* to reach another absorbing ^{57}Fe. Since $\Delta E/E$ = 2 MHz/3.5 x 10^{18} Hz is only one part in a trillion ($1/10^{12}$), the resonance is very sharp. If this source γ - ray (Fig 15.1) can be absorbed by a sample ^{57} Fe, a very sharp absorption would occur, except for a major problem due to Doppler broadening (or Doppler effect). If a stationary ^{57}Fe* emitted a γ - ray of such high energy, it would recoil with velocity u of $h\nu/m_{Fe}c$ which is about 100ms^{-1}. This recoil velocity u will cause a Doppler broadening of nu/c which will spoil the resonance condition entirely. One way to avoid Doppler broadening would be use large lattices so that the atoms in the lattice can not move. A better way is to move the source relative to the sample to counter the effect of Doppler broadening. The source is mounted on a support which can be moved at a few mm/s either by rotating a screw or electromagnetically. It is a stroke of good fortune that such small speeds are sufficient to match the emitter and the absorber levels. A motion towards the absorber (positive velocity) implies that the absorber levels have a larger separation than the source levels.

Example 15.1: Calculate the frequency shift between the emitter and absorber for the ^{57}Co source if the source is moved towards the sample at a speed of 1 mm/s.

Solution:

The Doppler shift is $\delta\nu = \nu\ v/c$ (15.1)

Frequency ν corresponding to 14.4 keV = (14400 eV x 8066 eV/cm) x c. Here eV is converted to cm^{-1} by using 1 eV = 8066 cm^{-1}. The product is multiplied by c (in cm/s) to get frequency in Hz.

$\delta\nu = \nu\ v/c = \nu \times 1.16 \times 10^8 (c/c)\ cm^{-1}$

$= 0.1(cm/s) \times 1.16 \times 10^8 cm^{-1} = 11.6$ MHz

So far, we have seen why the sample absorption can occur at a frequency other than source emission frequency. In Mossbauer spectroscopy, the change in the position of the resonance is often called the isomer shift (rather than chemical shift). The spectra are recorded as the γ - ray counting rate versus the velocity of the source. The other reason for isomer shifts is the difference in the s-electron density at the nucleus. Excited states of nuclei often shrink by a few percent on excitation. The change in the energy of the nuclear isotope

$$\Delta E \alpha \ \Psi_s^2(0)\ \delta R \qquad (15.2)$$

Here $\Psi_s^2(0)$ is the square of the electron density at the nucleus and δR the change in the nuclear radius. If the nuclear spin of the excited state is different from the ground state (eg I = ½ for ^{57}Fe and I = 3/2 for $^{57}Fe^*$), the quadrupole moment (resulting from spins >½) leads to quadrupolar splitting of the absorption frequency. The nuclear energies of spins 1/2 and 3/2 are different giving rise to two lines. In fig 15.2, the Mossbauer spectra of $Fe(CN)_6^{4-}$, $Fe[(CN)_5NO]^{2-}$ and $FeSO_4$ are shown.

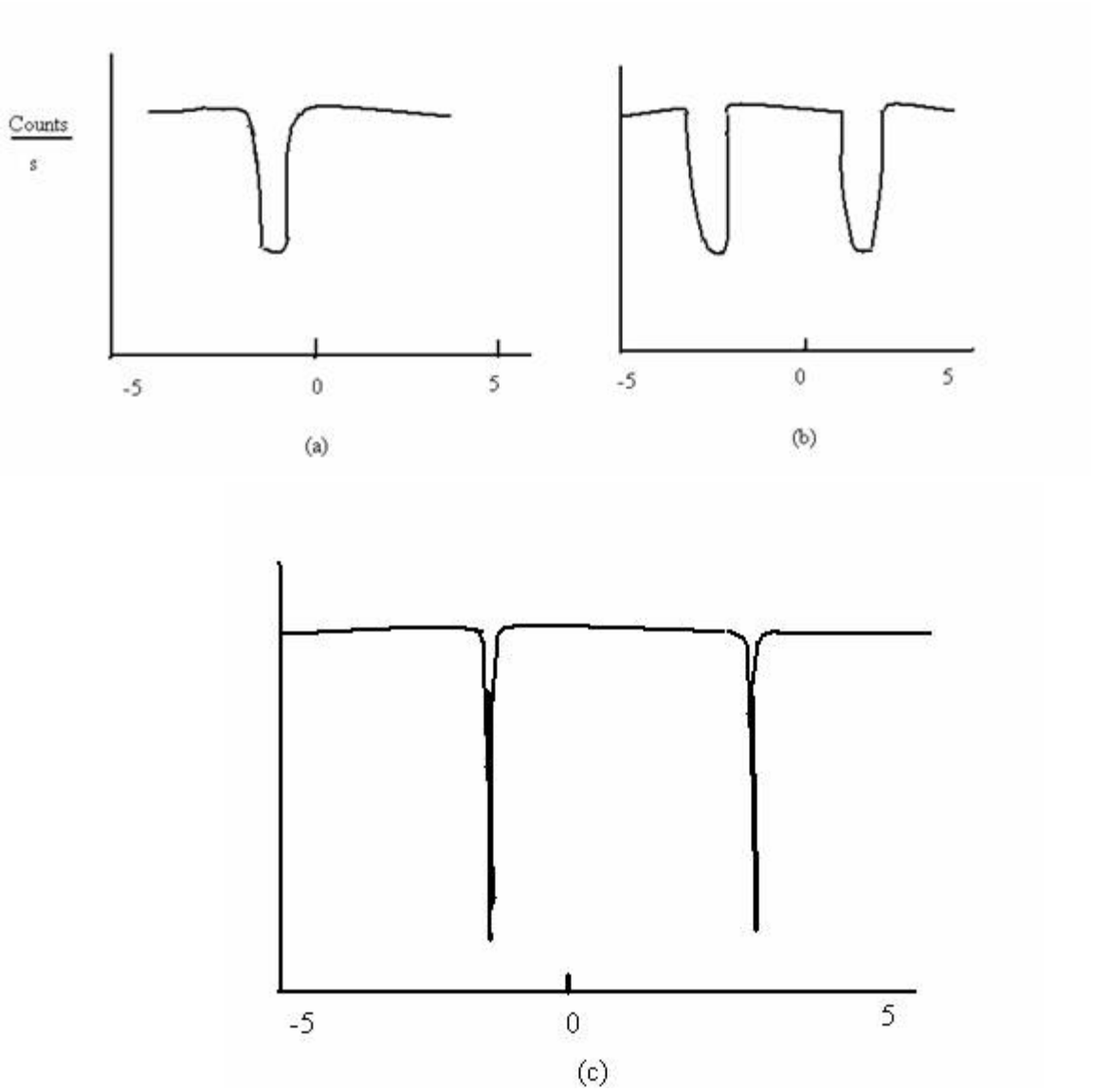

Fig. 15.2. Mossbauer spectra of $Fe(CN)_6^{4-}$, (a), $Fe[(CN)_5NO]^{2-}$, (b) and $FeSO_4$ (s) (c). For quadrupole moment to influence ΔE, there has to be an electric field gradient at the nucleus which is present in (b) and

(c) above because they possess sufficient asymmetry to possess electric field gradients at the nucleus. Spherical symmetry or perfect octahedral symmetry does not produce electric field gradients.

15.3 Nuclear Quadrupole Resonance (NQR) Spectroscopy

If two charges e and –e are separated by a distance d, they constitute an electric dipole of moment ed. The units are Debye (10^{-18} esu.cm), or in the MKS, Cm. (Coulomb meter). More extended charge distributions such as two + and two – charges separated from one another lead to a quadrupole moment eQ which is defined as

$$eQ = \int \rho(x,y,z)\, r^2\, (3\cos^2\theta - 1)\, d\tau \qquad (15.3)$$

Here, $\rho(x,y,z)$ is the charge density at r = (x,y,z), θ, the polar angle and $d\tau$, the volume of integration. Nuclei with spins $I \geq 1$ have a quadrupole moment. Nuceli with spins ½ do possess a dipole moment, but their quadrupole moment is zero as the +ve charge density contribution is cancelled by the –ve contribution in Eq. (15.3).

A point charge e interacts with the electrostatic potential V at its location to give an interaction energy eV. A "point" dipole μ interacts with the electric field E in which it is placed to give energy $-\mu.E$ The quadrupole interacts with the electric field gradient, whose components are given as the second derivative of the electrostatic potential

$$eq_{ij} = \partial V / \partial x_i\, \partial x_j \; ; \qquad x_i = x,y,z, \;\; x_j = x,y,z \qquad (15.4)$$

The quadrupole moment can be positive or negative, depending on the shape of the nucleus. Two cases are shown in Fig 15.3.

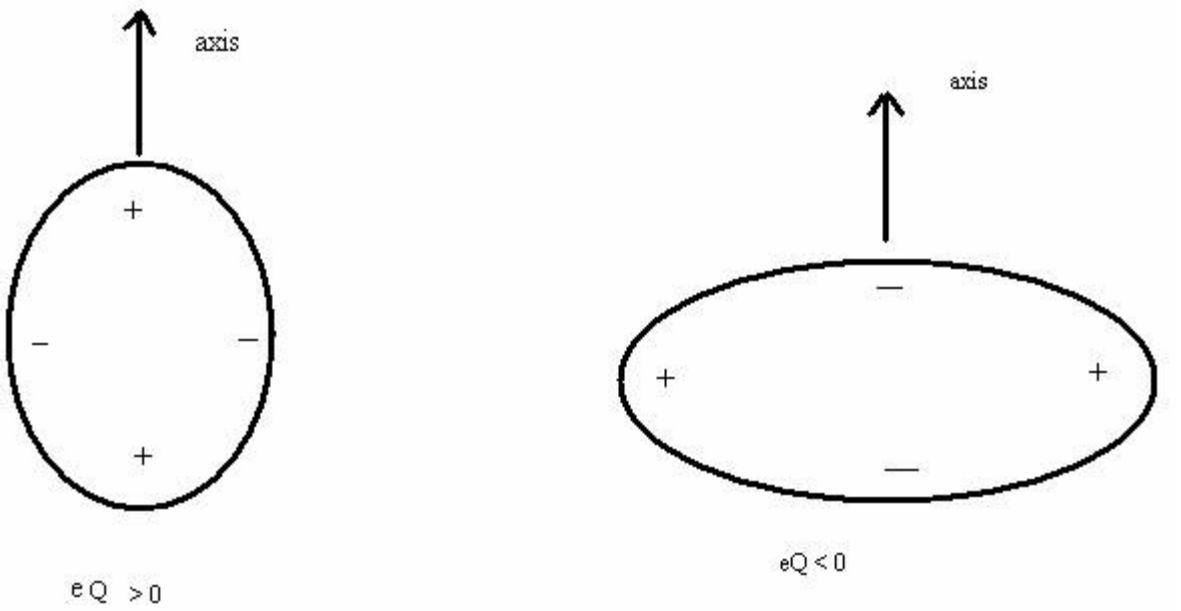

Figure 15.3. Nuclear spins with I ≥ 1 having positive and negative quadrupole moments.

In a liquid sample, molecular motion causes the electric field gradient to average to zero and NQR is observed only in solid samples. ^{14}N and ^{35}Cl are the common nuclei which exhibit NQR absorption in the frequency range of 20 – 40 MHz. For axially symmetric systems, the quantized energy levels due to the quadrupole-electric field gradient interaction are

$$E_m = e^2\, q\, Q\, [3\, m^2 - I\,(I+1) \,/\, 2I\,(2I-1) \qquad (15.5)$$

In the above equation, I is the nuclear spin quantum number, $q = \partial^2 V / \partial z^2$, the electric field gradient in the direction of the axis of symmetry and m, the projection of I is given by

$$m = I,\ I - 1,\ \ldots\ldots - I + 1,\ - I \qquad (15.6)$$

Note that the energy levels depends on m^2 and + m and – m values correspond to the same energy. The selection rule for an NQR transition is,

$$\Delta m = \pm 1 \qquad (15.7)$$

The frequency for a transition from m - 1 to m level is given by

$$\nu = \frac{3e^2 q\theta}{4I(2J-1)h} \quad (2|m|-1) \qquad (15.8)$$

The quantity e^2qQ/h is called the nuclear quadrupole coupling constant. The energy levels for spins 1, 1½ and 2½ are shown in Fig 15.4

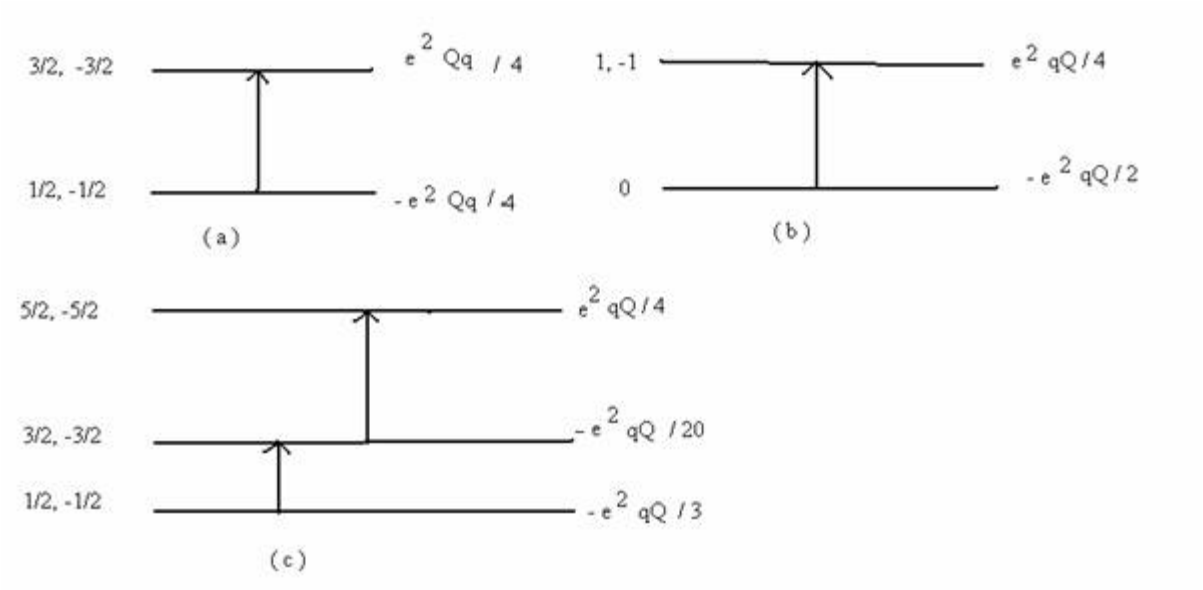

Figure 15.4. The energy levels for I = 1(a), I = 3/2(b) and I(5/2) (c) and the allowed NQR transitions.

For non axially symmetric systems, the energy levels deviate further and the degeneracy of the $m \neq 0$ levels is split. The energy levels are then expressed in terms of an asymmetry parameter $\eta = (q_{xx} - q_{yy})/q_{zz}$. In the NQR Spectrometer, the sample is placed in an inductance, L, which is tuned to the absorption frequency by varying the capacitance of the capacitors C, connected to L. The voltage output which is affected by the absorption is observed in an oscilloscope.

NQR can not be used as widely as NMR because of fewer $I \geq 1$ nuclei and the requirement of the solid state sample. However for compounds containing N and Cl, good use of NQR has been made to generate the molecular data for e^2qQ and η in different environments. In metal cyano complexes, the migration of the electrons of the central metal to the empty π^* orbitals of the cyano groups affects the field gradient values at ^{14}N. In the case of group III trihalides, the terminal halides in dimerised AlX_3 have different frequencies than the bridging halides.

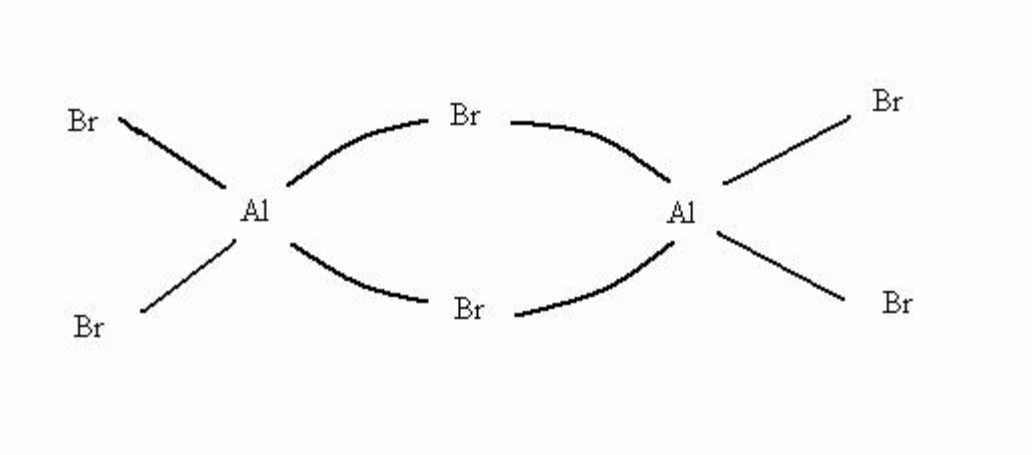

Figure 15.5. Structure of $AlBr_3$ dimer. The terminal bromines absorb at 113.79 and 115.45 MHz, while bridging bromines absorb at 97.945 MHz, Chlorides of I, Au and Ga absorb at lower frequencies.

The data on group frequencies of C-Cl can be used as an analytical tool. Values of C-Cl absorption frequencies in MHz for some groups are –COCl (29-34), O-C-Cl (19.7 to 32.7), C-Cl (31-43), CCl_2 (34.5 – 42.5), CCl_3 (38-42), S-C-Cl (33 to 34.6) and = C-Cl (36.5 to 39.5). Intermolecular hydrogen bonding reduces the field gradients at nuclei such as ^{35}Cl and ^{14}N by about 20% and this can be detected in NQR.

15.4 Raman Spectroscopy

In 1928, Raman observed that when monochromatic radiation was incident on molecules, most of the scattered light had the same frequency, ν_0 of the incident light (Rayleigh Scattering) and in addition, there were some discrete frequencies above and below the frequency of the incident beam. The process is refered to as Raman Scattering and the discrete lines are referred to as Stokes' and anti-Stokes' peaks. The additional lines are mainly due to the rotational and vibrational levels of the molecules.

You may recall from the earlier chapters that the rotational and vibrational spectra required the presence of the molecular dipole moment. In Raman Spectroscopy, the transitions are induced by the fluctuating molecular polarizability. Polarizability denotes the extent of possible distortion of the electron cloud in the presence of an external electric field. The induced dipole moment is defined by

$$\mu = \alpha E \qquad (15.9)$$

Tightly bound electron clouds such as those in F_2 have low polarizability while soft and weakly bound molecules like I_2 have large values of polarizability. Polarizability is a tensor. The physical meaning of the polarizability tensor is that a field in one direction induces distortions not only along the field direction, but also along the other two directions. Considering the 3 directions of the field (x,y,z), there will be nine components of polarizability which can be labeled as xx, xy, zz, yx, yy, yz, zx, zy, zz. Polarizability of nonspherically symmetric molecules is asymmetric. The polarizability of a molecule is represented as an ellipsoid. The polarizability ellipsoid of H_2 is shown in Fig. 15.6.

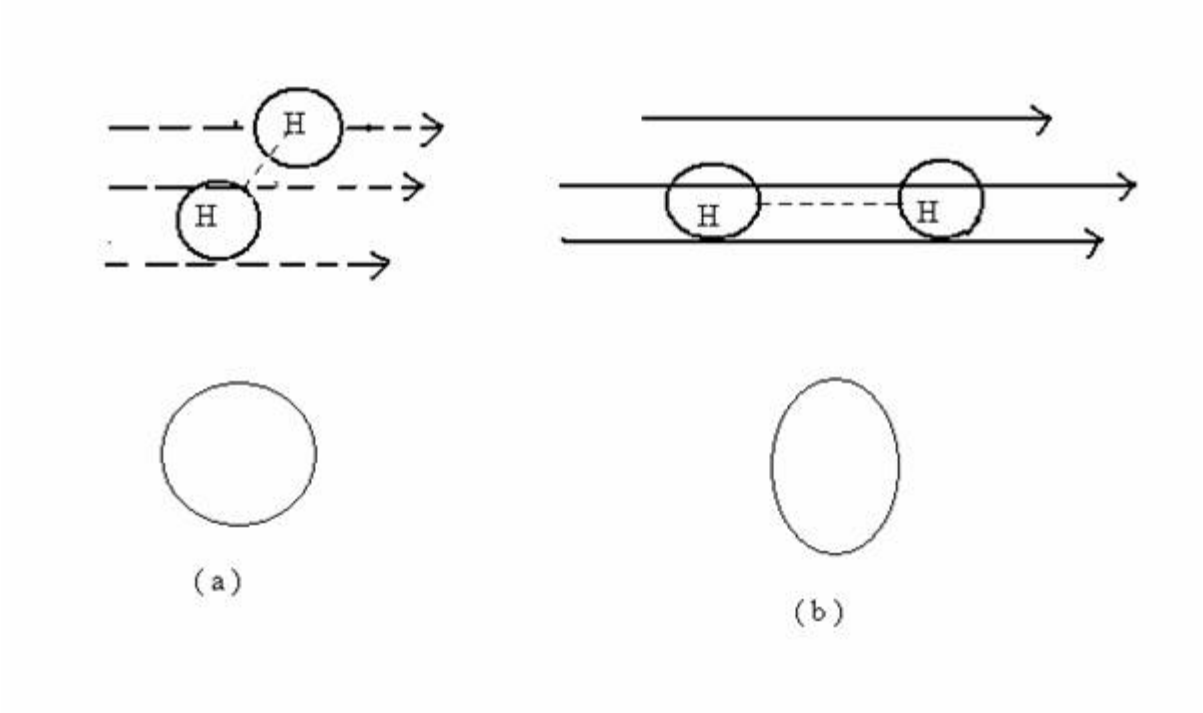

Figure 15.6. Polarizability ellipsoids of H_2, perpendicular to the bond (a) and parallel to the bond (b).

The polarizability ellipsoids of other linear molecules are similar to those of H_2. The ellipsoids are drawn to represent polarizability in a "reciprocal" manner. When the distance from the center of the ellipsoid to a point on the surface is greatest, polarizability along that direction is least. The radial distance of the ellipsoid to a point i, r_i is proportional to $1/\sqrt{\alpha_i}$ where α_i is the polarizability along that axis.

If α_0 is the polarizability at equilibrium and ß the maximum extent of the change in polarizability during the vibration, then, the polarizability changes during molecular vibrations as $\alpha = \alpha_0 + ß \sin 2\pi \nu_{vib} t$, where vvib is the vibrational frequency. Since the applied electric field also has the sinusoidal component oscillating at a frequency v, the oscillating dipole can be expressed as

$$\mu = (\alpha_0 + ß \sin 2\pi \nu_{vib} t). E_0 \sin 2\pi\nu t \qquad (15.9)$$

Reexpressing the product of sines,

$$\mu = \alpha_0 E_0 \sin 2\pi\nu t + ½ ß E0 \{\cos 2\pi(\nu-\nu_{vib}) t + \cos 2\pi(\nu + \nu_{vib})t\} \qquad (15.10)$$

Here E_0 is the amplitude of the applied field. We thus see that there are oscillating dipoles with frequency components $\nu \pm \nu_{vib}$.

The selection rule for Raman transitions are governed by the changes in the components of molecular polarizability during a rotation or a vibration.

Let us consider the rotational Raman spectra of linear molecules. Without considering the centrifugal distortion constant D, the energy levels are given by

$$\varepsilon_J = B J(J + 1) \text{ cm}^{-1}, \quad J = 0,1,2 \qquad (15.11)$$

The rotational Raman Selection rule is,

$$\Delta J = 0, \text{ or } \pm 2 \text{ only and} \qquad (15.12)$$

$$\Delta\varepsilon_J = E_{J+2} - E_J = B (4J+6) \qquad (15.13)$$

Recall that for pure rotational spectra, $\Delta J = \pm 1$. From Fig.15.6(a), it is seen that the rotation about the bond axis produces no change in the polarizability ellipsoid whereas the end over end rotation changes the ellipsoid. In every complete rotation, the molecular ellipsoid has the same appearance twice. The observed spectral lines appear at

$$\nu_{PR} = \nu_{ex} \pm \Delta\varepsilon = \nu_{ex} \pm B(4J + 6)\ cm^{-1} \qquad (15.14)$$

Here RR refers to rotational Raman.

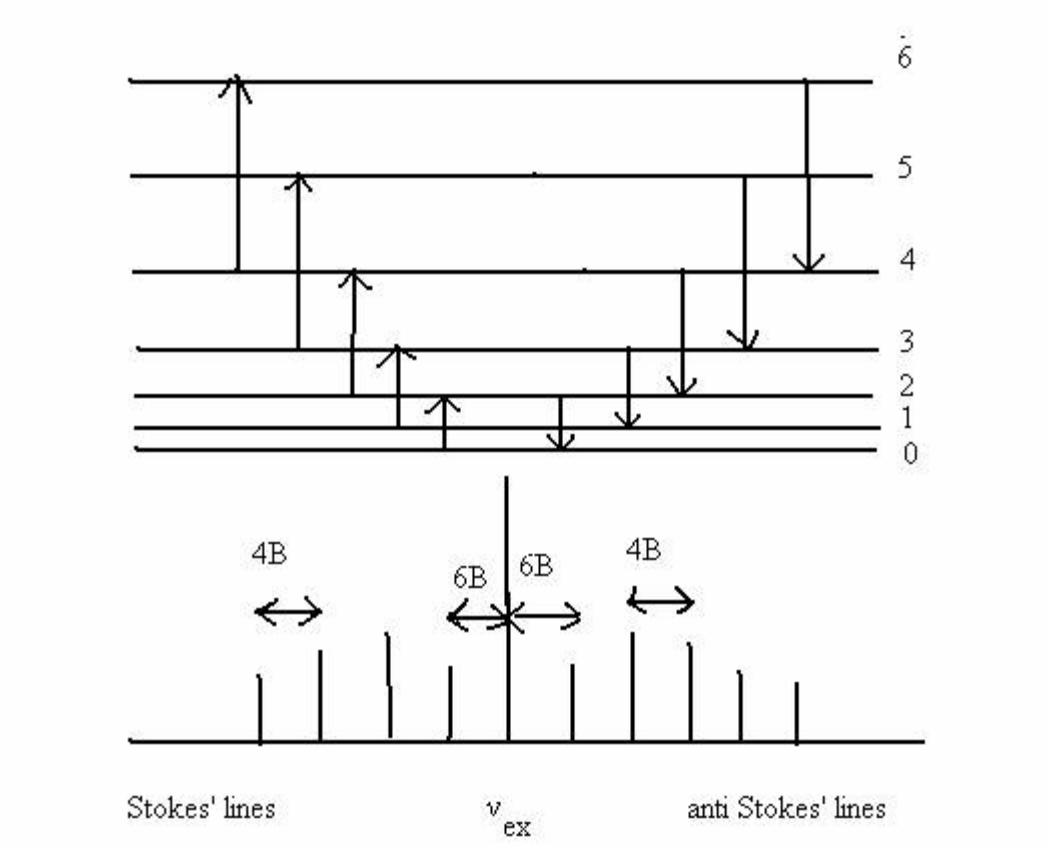

Figure 15.7. Rotational Raman Spectrum of a linear molecule.

The cases where centrifugal distortion is taken into account, and the extension to symmetric tops and other molecules can be analysed as in the case of pure rotational spectra. The selection rules for symmetric tops are different for $K = 0$ and $K \neq 0$.

We will now consider vibrational Raman Spectra. Let us recall that symmetric stretches were IR inactive because the molecular dipole moment did not change during this mode. But in case of symmetric stretch, the changes in the polarizability are more than in the case of asymmetric stretch or bending. The following figure shows these changes.

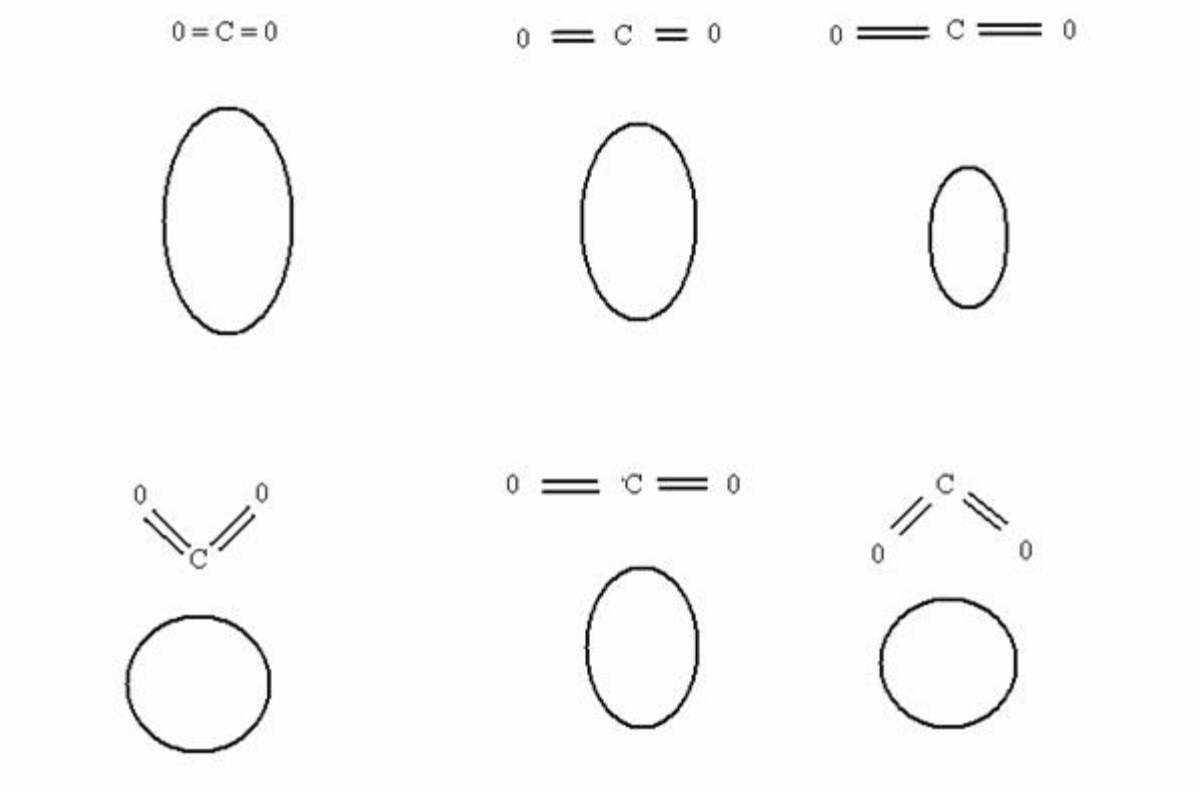

Figure 15.8. Changes in molecular polarizability during a symmetric stretch (a) and bending mode (b) of CO_2

The general rule for vibrational Raman Spectroscopy is that the symmetric vibrations give intense Raman lines and non-symmetric vibrations are weak or inactive. There is a rule of mutual exclusion: For a molecule having a center of symmetry, infrared active vibrations are Raman inactive and vice versa. For other molecules, both IR and Raman lines may be observed.

The selection rules for vibrational Raman Spectra are

$$\Delta\nu = 0, \pm 1, \pm 2 \text{ and} \qquad (15.15)$$

$$\nu = \nu_{ex} \pm \Delta\varepsilon_{vib} \qquad (15.16)$$

These vibrational Spectra may also show a rotational fine structure with the $\Delta J = 0, \pm 2$ selection rule.

15.5 Time Resolved Spectroscopy

Modern laser techniques allow us to generate pulses of the order of femtoseconds. Additional details on lasers and time resolved spectroscopy will be given in the lectures on kinetics. Reaction dynamics and ultrafast spectroscopy are nicely interwoven as the latter provides the techniques to study the former. Activated complexes which are the short lived intermediates between the reactants and products are very short lived. At most, they undergo a few vibrations and a few rotations if they are sufficiently long lived and decay into products. To study the time domain behaviour of these short lived species, we need two pulses of laser light. The first is the pump pulse which initiates the reaction. The second one is the probe pulse which is flashed through the reaction mixture at several delayed time steps to probe the extent of changes occurring in the reaction.

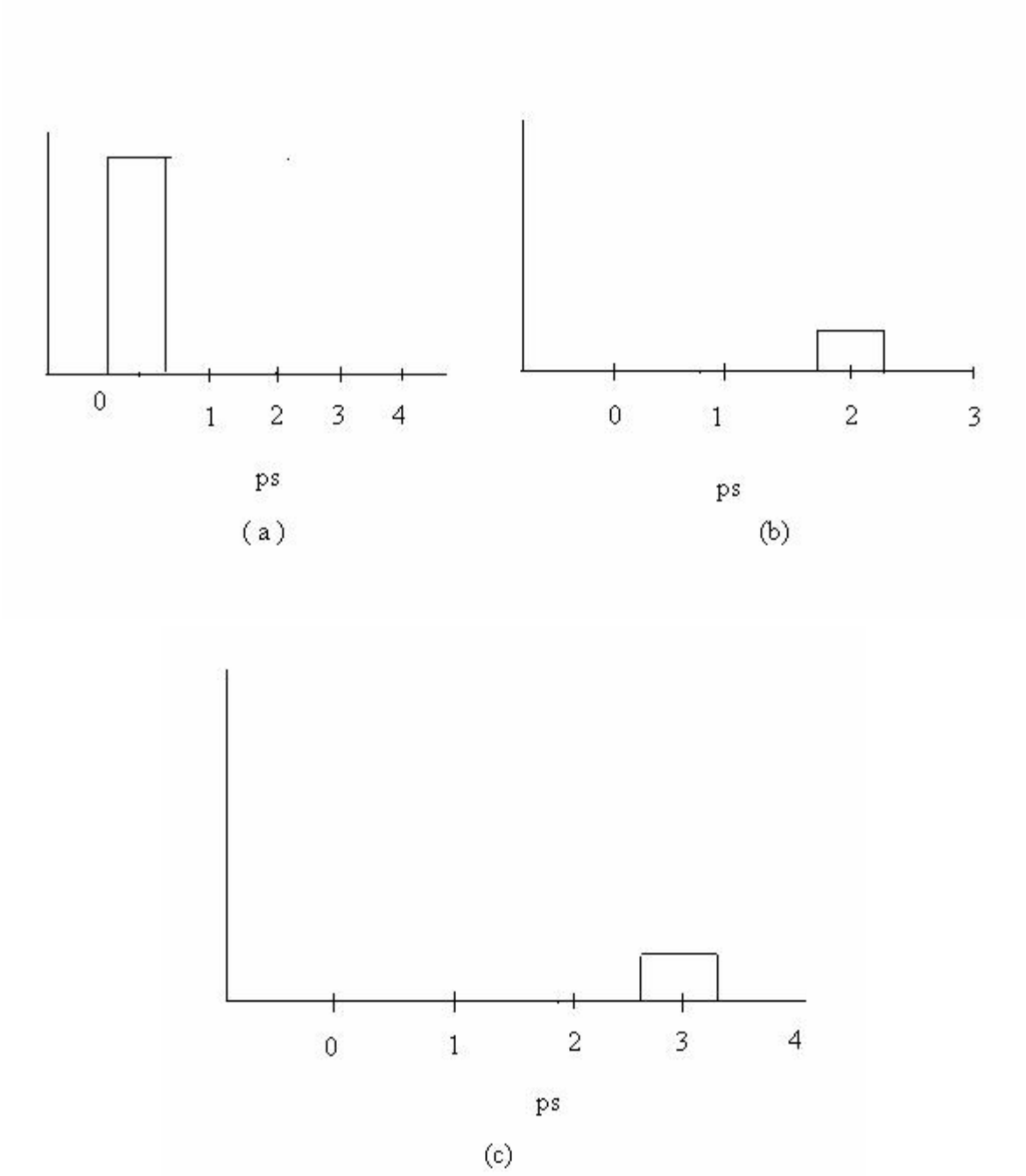

Figure 15.9. Sketches of a pump pulse (a) and probe pulses (b) and (c).

Molecular dissociations and bimolecular reactions have been studied by these methods. The dissociation of NaI has been described in the kinetics section. We will briefly describe the bimolecular reaction of HI with OCO. Molecular beams of HI and CO_2 are produced and are made to intersect. Weak complexes called the van der Waals complexes are formed. In the present case, the complex is I - H...OCO. The H....O distance is much longer than the OH bond distance in water or alcohols. By the use of a femtosecond pump pulse, the HI bond is broken. The H atom now moves closer to the oxygen to form the activated complex [HOCO]*. The probe pulse is "tuned" to a suitable frequency of the OH radical. Using this probe, the following dissociation process can be studied

$$HI + OCO \rightarrow IH...OCO \rightarrow [HOCO]^* \rightarrow HO + CO \qquad (15.17)$$

15.6 Mass Spectrometry (Spectroscopy)

Mass Spectrometry (Spectroscopy) does not involve transitions between energy levels. In this method, molecular ions are generated by ionizing the molecule ($M \rightarrow M^+$) The ion M^+ is called the parent ion.

During the ionization process, the molecules get fragmented resulting in'daughter' ions, M_i . All these ions are passed through a magnetic field which separates different ions depending on their mass/charge ratio. Combining the Newtons law (F=ma) and the Lorentz law (F = qE + v x B) , where m is the mass, q, the charge, v, the velocity E the electric field and B, the magnetic field, the particle's motion as a function of time is determined by the following combined equation.

$$(m/q)a = E + v \times B \qquad (15.18)$$

A block diagram of a mass spectrometer is shown below.

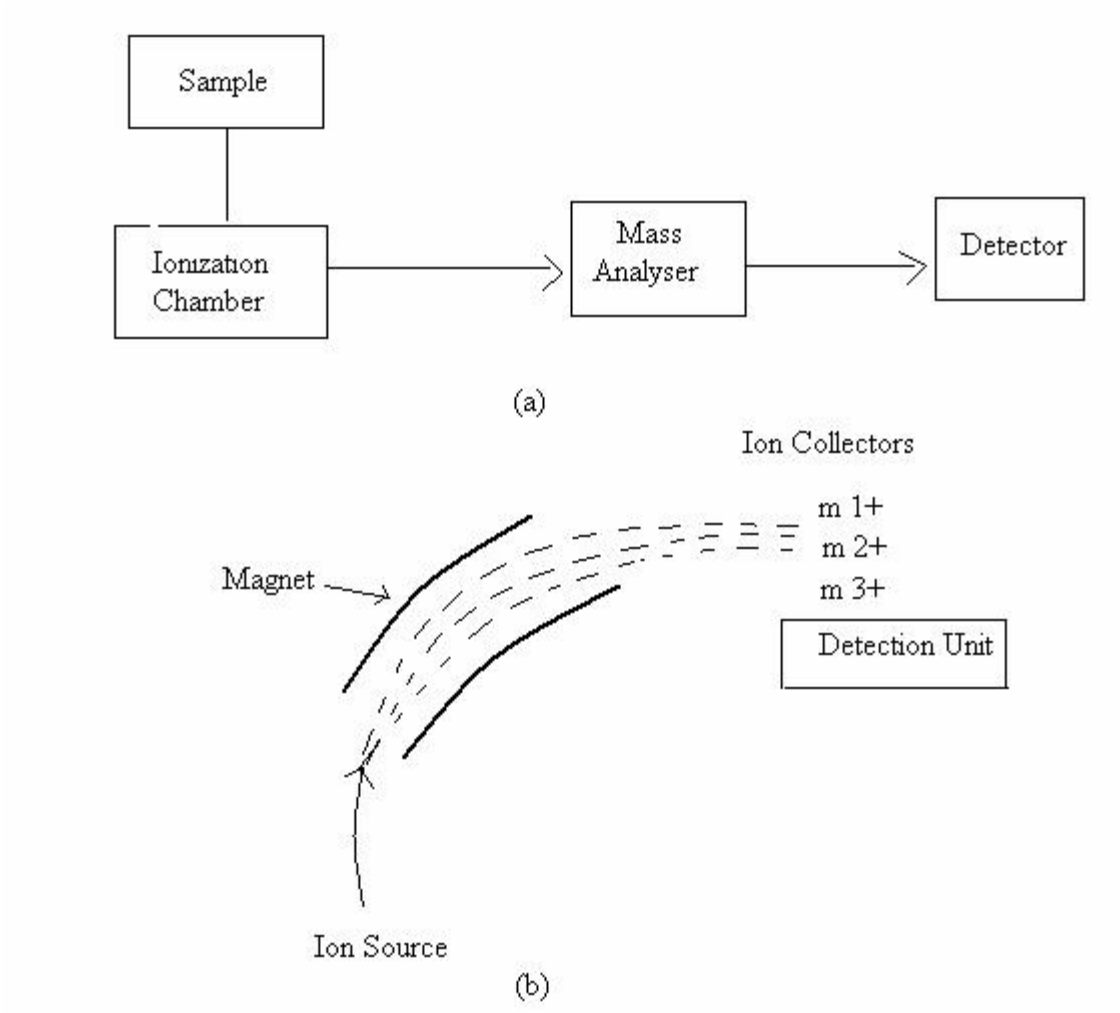

Figure 15.10. Block diagram of a mass spectrometer (a) and a deflecting magnet (b) separating different M_i^+/q

We will consider a couple of examples of mass spectra. Mass spectrum of methane is expected to give peaks corresponding to CH_4^+, CH_3^+,CH_2^+ and CH^+. All peaks do not have equal intensities. The stablest ion has the largest intensity and for comparison with other peaks, this intensity is set to 100%. Ethane will show peaks at $C_2H_6^+$, $C_2H_5^+$, CH_3^+ (intense). CCl_4 shows corresponding to CCl_4^+, CCl_3^+, CCl_2^+ and CCl^+ . The major peaks in the dissociation of n-decane are at 142 (I=0.05), 113 (I=0.05), 99 (I = 0.08) 85 (I = 0.2), 71 (I = 0.35) 57 (I = 0.85), 43 (I = 0.1) and 29 (I = 0.22). Here, I corresponds to the relative intensity. A "fine structure" corresponding to the loss of one or two hydrogen atoms is also observed. A sketch of the mass spectrum is given in Fig. 15.11.

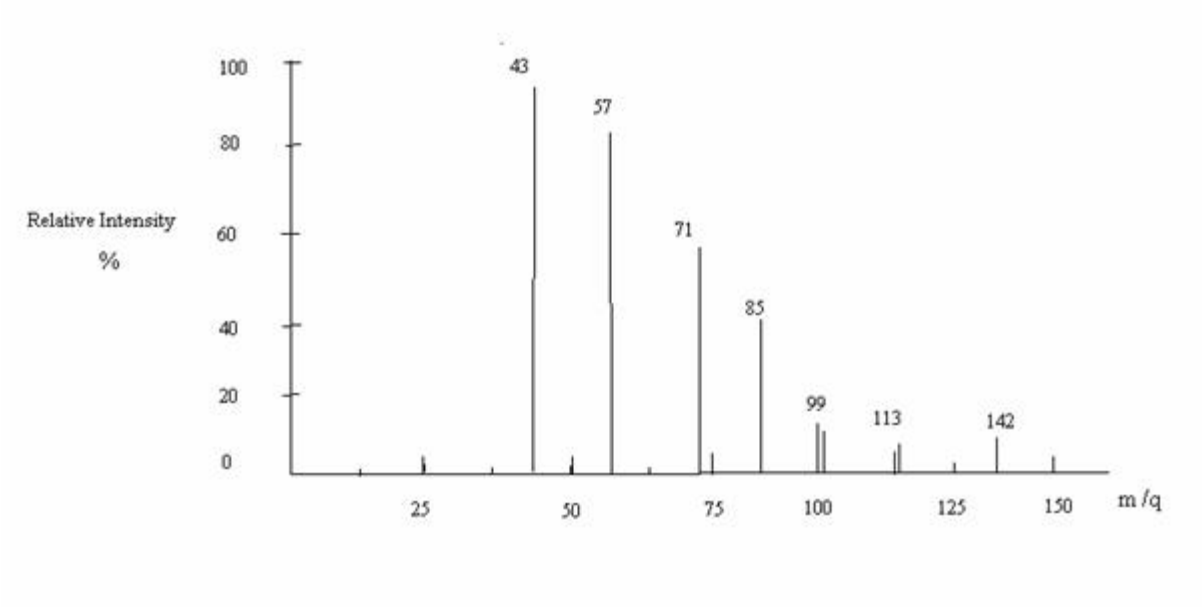

Figure 15.11. A sketch of the Mass Spectrum of n-C_{10} H_{22}

The peak at 142 corresponds to $C_{10}H_{22}^{+}$. A loss of C_2H_5 gives a peak at 113 ($C_8H_{17}^{+}$). Stepwise losses of CH_2 (14 atomic mass units, u) groups give peaks at 99, 85, 71, 57, 43 and 29. The last one corresponds to $C_2H_5^{+}$. Other peaks at 27, 41, 55, 56, 69, 70, 84, 98 and 112 are also seen (not shown in Fig 15.) The intensity of the peaks is difficult to predict a-priori and these depend on the stabilities of the structures. In the above spectrum, $C_3H_8^{+}$ is the most stable and long lived ion. Analysing mass spectra can actually be whole lot of fun.

Example 15.2 Rationalize the peak structure of the mass spectrum of $CH_3CH_2CH_2Br$ (1-bromopropane).
Solution. Br has two isotopes of mass 79 and 81 and both have nearly the same abundance. Parent molecular ions are observed at m/q of 122 and 124. The loss of ^{79}Br from the molar mass of 122u gives a base peak at 43 for the ion $CH_3CH_2CH_2^{+}$. The sketch of the spectrum is shown in Fig 15.12.

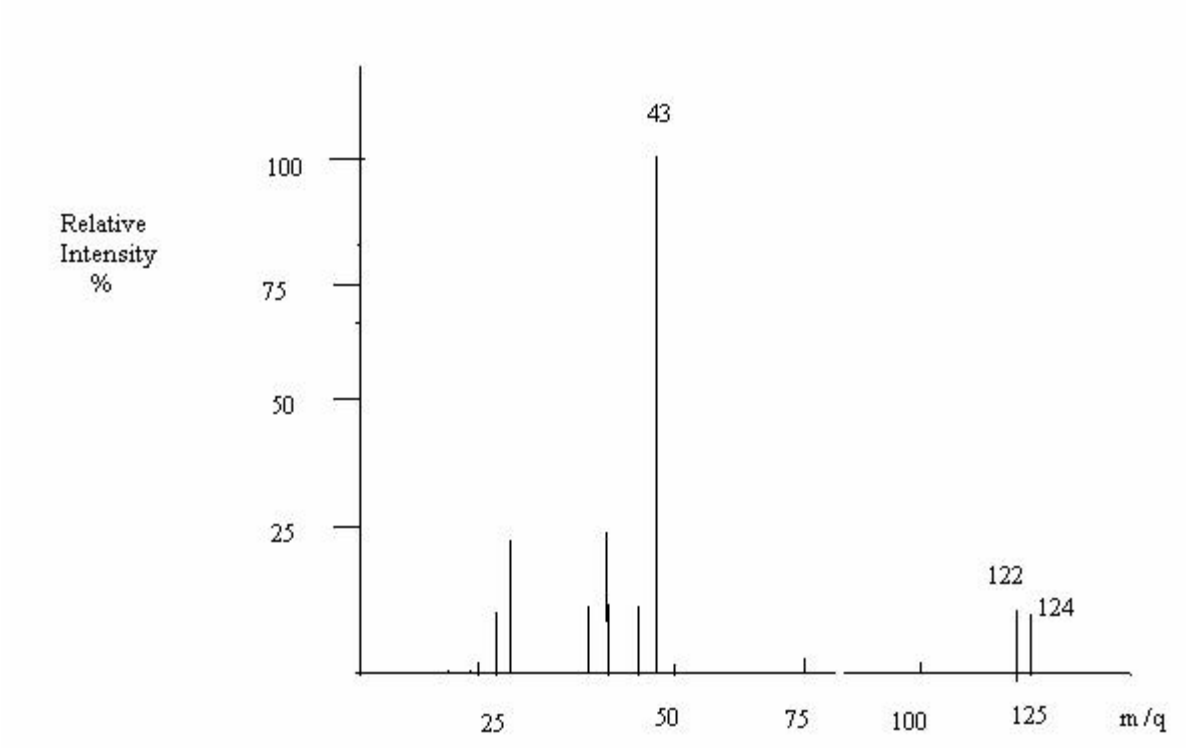

Figure 15.12. A sketch of the mass spectrum of $CH_3\ CH_2\ CH_2\ Br$.

Problems

1. A nucleus of mass 1.67 x 10^{-25} kg emits a γ - ray of 0.1 nm wavelength λ. The linear momentum of a photon is given by h/ λ. Calculate the recoil velocity of the nucleus, the Doppler shift and the frequency/wavelength of the γ - ray to a stationary observer.

2. How do the Mossbauer energy levels of ^{57}Co, ^{57}Fe and $^{57}Fe^*$ get affected by the application of an external magnetic field?

3. Show that the NQR coupling constant corresponds to a frequency.

4. Verify the values of ΔE given in Fig. 15.4.

5. In methane and acetylene, comment on the vibrational/Raman activity of different modes of vibration.

6. How will Fig. 15.7 change when centrifugal distortions are taken into account?

7. Sketch the approximate polarizability ellipsoids of the asymmetric vibration of CO_2.

8. Outline the time resolved spectrum of NaI.

9. Taking the bend length of H_2 to be 0.7417angstrom, sketch the rotational frequencies in a suitable Spectroscopic method.

10. Predict the mass spectra of the following molecules i) CH_3COCH_3 2) H_2O c) $C_6HsCONH_2$ and d) the three pentanes.

Recap

In this lecture you have learnt the following

15.8 Summary

In the present lecture, you have been introduced a few additional spectroscopic methods. Some of the equipments in ultrafast spectroscopy are so widespread that the small sample containing the molecules is a tiny intruder. We also hardly considered the effects of electric and magnetic fields (Stark and Zeeman effects) in spectroscopy. The methods considered here are Mossbauer spectroscopy, NQR, Raman spectroscopy, time resolved spectroscopy and Mass spectrometry. In Mossbauer spectroscopy, there is a reabsorption of an emitted γ-ray by the sample. The effects of Doppler broadening are negated by moving the source relative to the sample. In NQR, there are absorptions between the energy levels which come about by the interaction of the nuclear spin ($I \geq 1$) with the electric field gradients at the nucleus. In Raman spectroscopy, fluctuating molecular polarizability interacts with the incident beam to give scattered light at frequencies corresponding to rotational and vibrational energy differences. Time resolved spectroscopy uses pump probe techniques to excite a molecule (pump pulse) and then study the time evolution of the products and activated complexes through the probe pulse. In mass spectrometry (which is not traditional spectroscopy but a great analytical tool to study molecular structures) ionization of molecules and the fragments therein enable us to identify molecular structures precisely.